
TREATMENT-RESPONSE ANALYSIS OF TUMOR AS A QUANTUM PARTICLE

Nam Nguyen
Tampa, FL 33620
harveyng.510@gmail.com

May 4, 2023

ABSTRACT

In this article, I present a novel and computational-efficient approach for treatment-response modeling of tumor progression-free survival (PFS) probability using the physical phenomenon of a quantum particle walking on a one-dimensional lattice with the presence of a proximate trap.

1 Introduction

This paper presents a novel approach to the treatment-response analysis of tumors by introducing the theory and concept of a quantum survival model, which views tumors as quantum particles. I identify the potential use of the physical phenomenon of a quantum particle on a 1D lattice with the presence of proximate traps for treatment-response modeling. I will begin with outlining the limitations of classical, non-parametric survival analysis in **Section 2.1**. Next, I will explain the progression-free survival (PFS) analysis from both classical and quantum random walk perspectives in **Section 2.2**. **Section 3** translates the theory and concept of the quantum survival model in the context of treatment-response modeling. In contrast, **Section 3.4** introduces an efficient model implementation on advanced classical computers. Finally, I will demonstrate the proposed model on Pan-Cancer PFS analysis using The Cancer Genome Atlas (TCGA) database [1], which includes a large dataset of approximately 10,000 samples. This work's primary contribution is applying quantum algorithms for biomedical research, providing new insights into tumor progression as a quantum particle.

2 Preliminaries

2.1 Limitation of Kaplan–Meier Survival Analysis

The Kaplan-Meier (KM) estimator [9] is a non-parametric statistic used to estimate the survival function of a population or a group of individuals, one of the most dominant models in medical research. The model enables the estimation of the survival probability of patients, study participants, or systems over time. The KM estimator is given by

$$\hat{S}(t) = \prod_{t_i \leq t} \frac{n_i - d_i}{n_i}, \quad (1)$$

where $\hat{S}(t)$ is the Kaplan-Meier estimate of the survival probability at time t , t_i is the time of the i^{th} event, n_i is the number of individuals at risk just before the i^{th} event, and d_i is the number of individuals who experience the i^{th} event.

I realize that KM-based survival models have three major limitations, which are given as follows:

1. **Censoring and proportional hazards assumption:** One of the major limitations of KM analysis is the Censoring of data. Censoring occurs when the event of interest has not occurred in some participants or their follow-up time ends before the event occurs. This leads to incomplete information and may affect the accuracy of the results. Besides, KM analysis assumes that the hazard ratio is constant over time, which may not always be true. If the hazard ratio changes over time, the results of KM analysis may not be reliable.

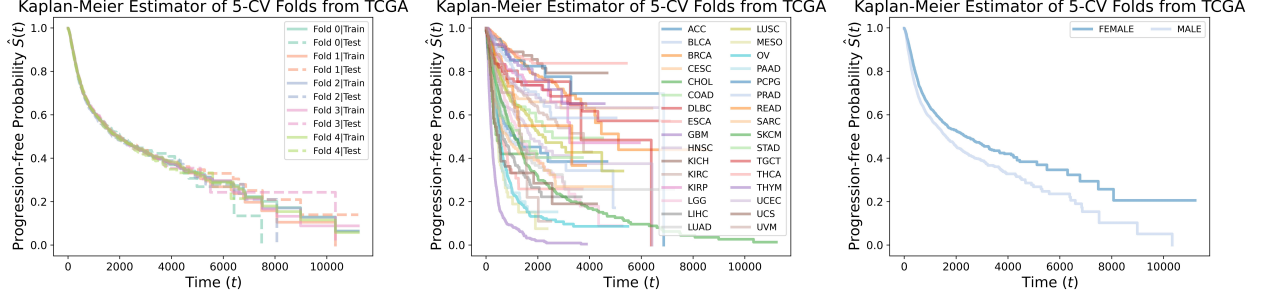


Figure 1: **KM Analysis of Progression-free Probability on TCGA Dataset [1].** Group comparison by gender (right panel) is more robust than comparison by cancer type due to sample size per group (middle panel). Besides, the model interpretation of such a non-parametric is low since it only provides an overall progression-free chance on the entire cohort (left panel).

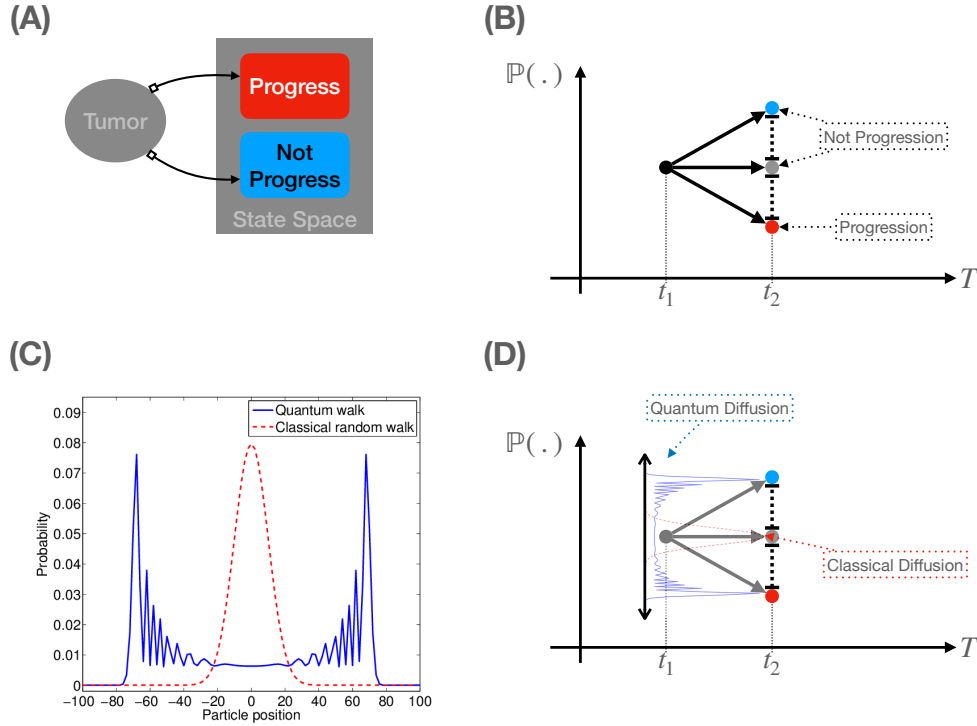


Figure 2: **Tumor Progression as Classical and Quantum Random Walks.** (A) Tumor progression state space, in which each tumor has only two future possibilities: (1) progression and (2) not progression. (B) Prediction surface of progression-free probability associated with tumor state space. (C) Classical v.s. Quantum Walks, figure credit from [4]. (D) Progression-free probability interpreted by quantum and classical diffusion.

2. **Sample size and group comparison:** The sample size can affect the accuracy and reliability of the results. If the sample size is too small, the results may not be statistically significant. Moreover, KM analysis can compare survival curves between different groups. However, the comparison may not be appropriate if the groups have different baseline characteristics that may affect the event of interest (Figure 1(middle and right panel)).
3. **Low level of model explainability:** The model cannot explain model inference via parameters since it is a non-parametric model (Figure 1(right panel)).

2.2 Classical v.s. Quantum Random Walks in the Context of PFS Analysis

I show the state space of a given tumor in **Figure 2(A)**, in which each tumor has only two future outcomes, either progress or not-progress. The prediction surface of progression-free probability associated with the state space is given in **Figure 2(B)**. Specifically, progression-free survival (PFS) refers to the period, including during and after the treatment of a disease, during which a patient lives with the disease, but it does not worsen. The measurement of PFS probability (in $[0,1]$) in a clinical trial is used to determine the efficacy of a new treatment.

The progression-free probability of a disease is directly related to tumor progression. In cases where the progression-free probability is high (**Figure 2(B)**), it could imply that the disease is not advancing. Thus the current treatment is effectively controlling or slowing down its growth. On the other hand, when the progression-free probability is low, it could imply that the tumor is growing and advancing despite the current treatment.

Hence, measuring the PFS in a clinical trial is one way to assess the efficacy of a new treatment for a disease, especially in cancer cases, and to determine whether it can effectively control tumor progression. A high progression-free probability is a positive outcome, suggesting the patient responds to treatment. In contrast, the low progression-free probability is a negative outcome, indicating that the treatment is ineffective in controlling tumor progression.

I associate the change in PFS probability with stochastic processes, which can be classical or quantum random walks (**Figure 2(C)** and **(D)**). Classical random walk is a stochastic process in which a particle or walker moves randomly in a one-dimensional space, either to the left or right, with equal probability. At each time step, the particle moves one step in either direction with a fixed probability. The position of the particle after a certain number of steps is determined by the random outcomes of each step. The classical random walk is described by classical probability theory, and the walker's motion is deterministic and entirely predictable.

Quantum random walk, on the other hand, is a stochastic process that describes the behavior of a quantum mechanical system consisting of a walker and an environment. In quantum random walk, the walker is described by a quantum state that is a superposition of all possible positions in a one-dimensional space. The walker's position is determined by the measurement of the walker's quantum state. Unlike classical random walk, quantum random walk is governed by quantum probability theory, which allows for interference between different paths, leading to different behavior and properties compared to classical random walk.

I observe that a classical random walk follows a normal distribution (**Figure 2(C)**), centralized around the initial position. In contrast, quantum random walks have a diffused distribution for particle position as the tumor is in the superposition, meaning it is simultaneously progressing and not-progress at the same time before measurement. Of note, quantum information is collapsed into classical information after the measurement.

3 Methods

3.1 Treatment-Response Modeling by Enticing Quantum Particle with Proximate Trap

Given a particle propagating on a 1D lattice with an initial position of α and a trap placed at the origin. The strength of the trap is tunable with parameter γ ; i.e., I can amplify the trap's strength to entice the particle. With the trap, the wavefunction $|\psi_{[n]}(t)\rangle$ of the quantum particle located at site n at time t follows the time-dependent reduced tight-binding equation [11]:

$$i\frac{d|\psi_n(t)\rangle}{dt} = |\psi_{n+1}(t)\rangle + |\psi_{n-1}(t)\rangle - i\gamma\delta_{n0}|\psi_0(t)\rangle, \quad (2)$$

where δ_{0n} is Dirac delta function.

The physical phenomenon induces a paradoxical observation: the survival probability of a particle can increase as the strength of the trap increases, even if the particle is proximate to the trap. Specifically, the top panel of **Figure 3** shows the dynamics with extremely large trap strength of $\gamma \in [0, 100]$ placed close to the quantum particle with $\alpha \in [0, 1]$. It is observed that with increasing trap strength, the particle has an increased chance to be survived, which is paradoxical (Quantum Zeno effect [11]) since the particle should have a greater chance of being trapped (not survive) in this scenario.

Here, I will explain the usage of such a quantum phenomenon in the context of treatment-response modeling for tumor progression. I associate the initial location α of quantum particles with **patient indicators** (normalized in $[0, 1]$) and the trap strength γ as the **treatment effect**. Of note, the discussed paradoxical phenomenon makes sense in treatment-response modeling. In particular, increasing trap strength means amplifying treatment effects, increasing particle survival chances. By Associating the particle survival with PFS, it can be interpreted that increasing treatment effect leads to higher PFS, and so the tumor does not progress (**Figure 2(B)**).

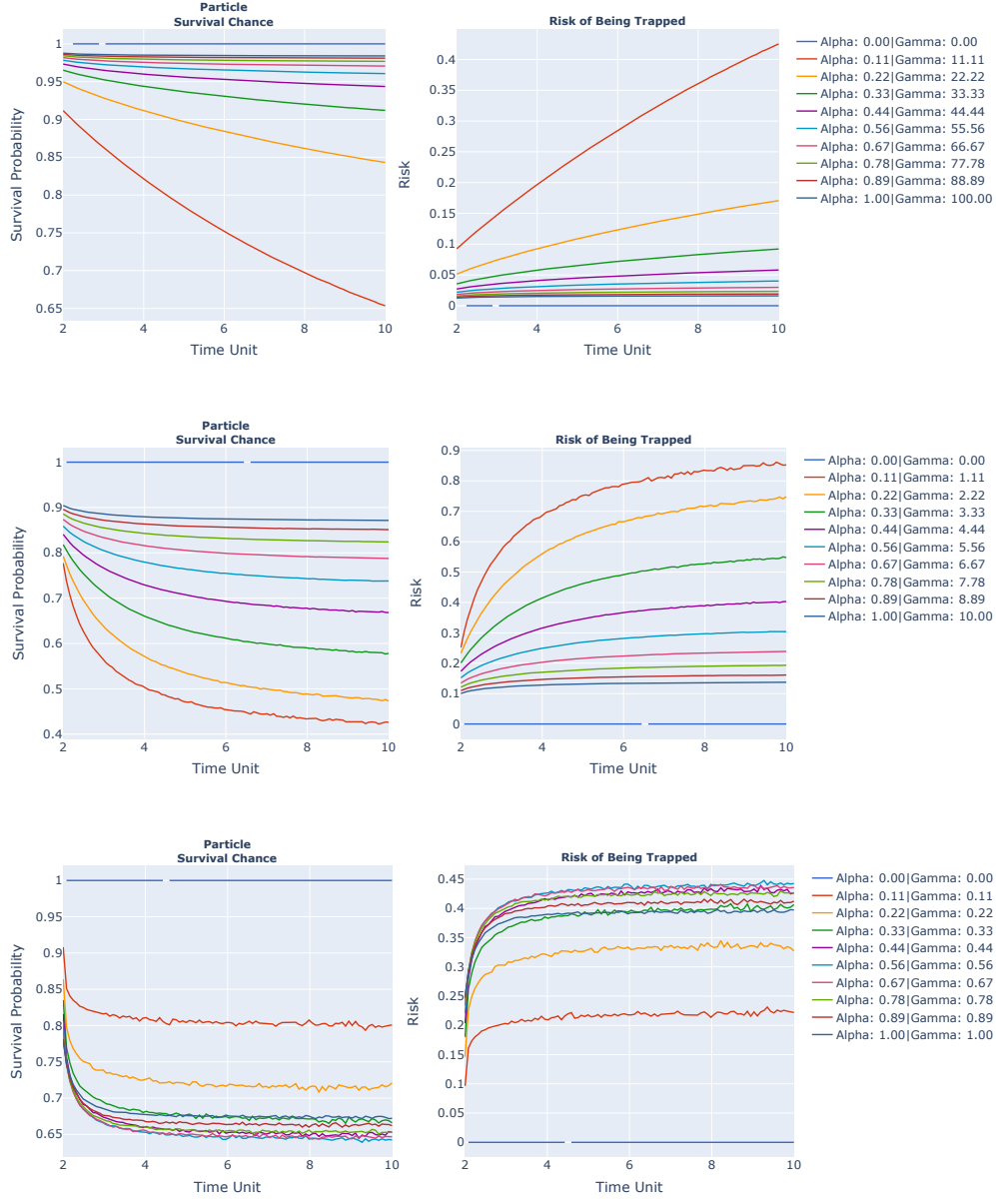


Figure 3: **Survival Probability of Quantum Particle Walking on 1D Lattice with the Presence of Proximate Trap.** I show the decreasing trap strength from the range $[0,100]$ (top), $[0,10]$ (middle), and $[0,1]$ (bottom).

3.2 Survival Probability and Risk Functions

The time-dependent survival probability function of the particle or tumor concerning trap strength γ is given by [11]

$$S(t|\gamma, \alpha) = 1 - 2\gamma \int_0^t |\psi_0(u)|^2 du = 1 - 2\gamma I = A(\gamma) + B(t|\gamma, \alpha), \quad (3)$$

where $|\psi_0(u)|^2 = \langle \psi_0(u) | \psi_0(u) \rangle$ is the statistical interpretation of particle wavefunction [7]. The main result of the work [11] shows that such probability can be computed by using

$$I = A(\gamma) + B(t|\gamma, \alpha) \quad (4)$$

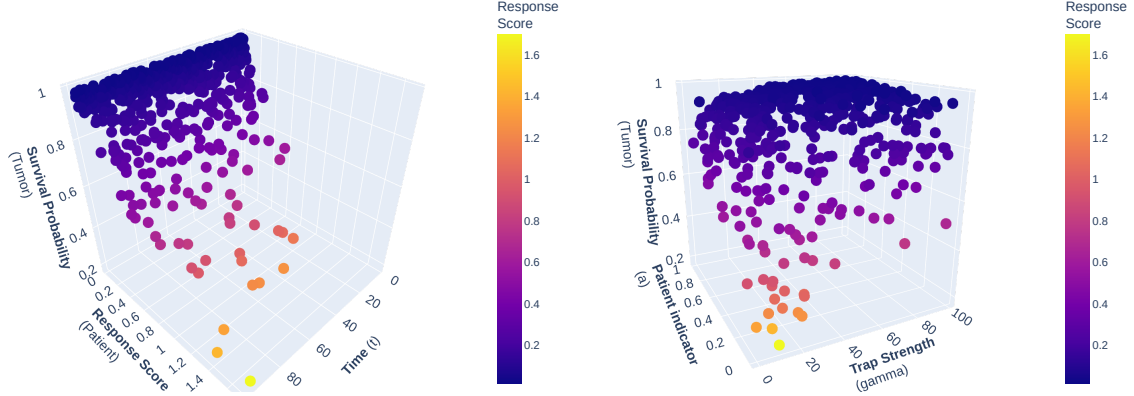


Figure 4: **Model Interpretation for Treatment Response Modeling Using Patient Indicator (Initial Position of Particle (α)) and Treatment Effect (Trap Strength (γ)).** (Left) Simulation results of the proposed model with $\gamma = 3, \alpha = 2$; monitoring time is from time 2 \rightarrow 100 (time unit) with 500 observations over the timeline. (Right) Survival probability of the particle with respect to patient indicator α and trap strength γ .

where

$$A(\gamma) = \frac{1}{\pi} \int_0^2 \frac{du}{(\gamma + \sqrt{4 - u^2})^2} \quad (5)$$

and

$$B(t|\gamma, \alpha) = \frac{1}{\pi} \int_2^t \frac{du}{\gamma^2 + u^2 - 4} \left(\frac{u - \sqrt{u^2 - 4}}{2} \right)^{2\alpha} \quad (6)$$

Fitting the survival model $S(t|\gamma, \alpha)$ is generally challenging with classical computing. Specifically, simulating quantum phenomena with classical computers is generally inefficient [10]. The computation of integration terms is based on numerical approximations enabled by sampling methods, which may induce significant errors when computing the hazard (risk) function $\lambda(t|\gamma, \alpha) = -\frac{d}{dt} \log S(t|\gamma, \alpha)$.

I propose a new metric to measure the treatment response score of an individual patient using the proposed model. Specifically, conventional survival analysis concerns the survival time of a patient, which coins the terms risk or hazard rate of this patient. In contrast, my work examines the tumor's survival concerning certain treatment effects. As a result, the term "risk" becomes the tumor risk under the given treatment, which can be hypothesized to correlate negatively with patient risks. This biologically makes sense since the risk of the tumor getting cured (trapped) should be highly associated with the response effect of treatment on the patients. Hence, I will further denote the approximated risk of a tumor, i.e., response scores of patients as

$$\rho(t) = \lambda(t) = -\log S(t). \quad (7)$$

It is worth noting that the proposed patient response score $\rho(t)$ will be positive real numbers as the negative logarithm of value in $[0, 1]$. Besides, the proposed model requires time calibration $t_{\text{model}} = t_{\text{actual}} + 2$ to avoid non-sense computation of term $B(t|\gamma, \alpha)$ in the survival function; i.e., the upper-bound of the integral must be greater than lower-bound since I are modeling tumor as quantum particle forward in the timeline.

3.3 Explainability of Model

I can explain the model prediction surface using the two hypothesized parameters (γ, α) used in the model as in **Figure 4**. Similar observations as discussed previously illustrated in the plot: proximate trap with a small is prone to have a better response. Nevertheless, the response effect will be maximal at some trap strength value γ ($t = 10 \rightarrow 20$ in the right panel of **Figure 4**).

3.4 Efficient Implementation of Quantum Simulation on Advanced Computing Hardware

I assume that for a quantified cohort of interest, I can find an optimal value for the two parameters (γ, α) that yields the maximum likelihood for this data of interest. Specifically, I re-formulate the loss function as

$$\mathcal{L}(\gamma, \alpha) = \text{ConcordanceIndex}(\rho(t), I_i) \quad (8)$$

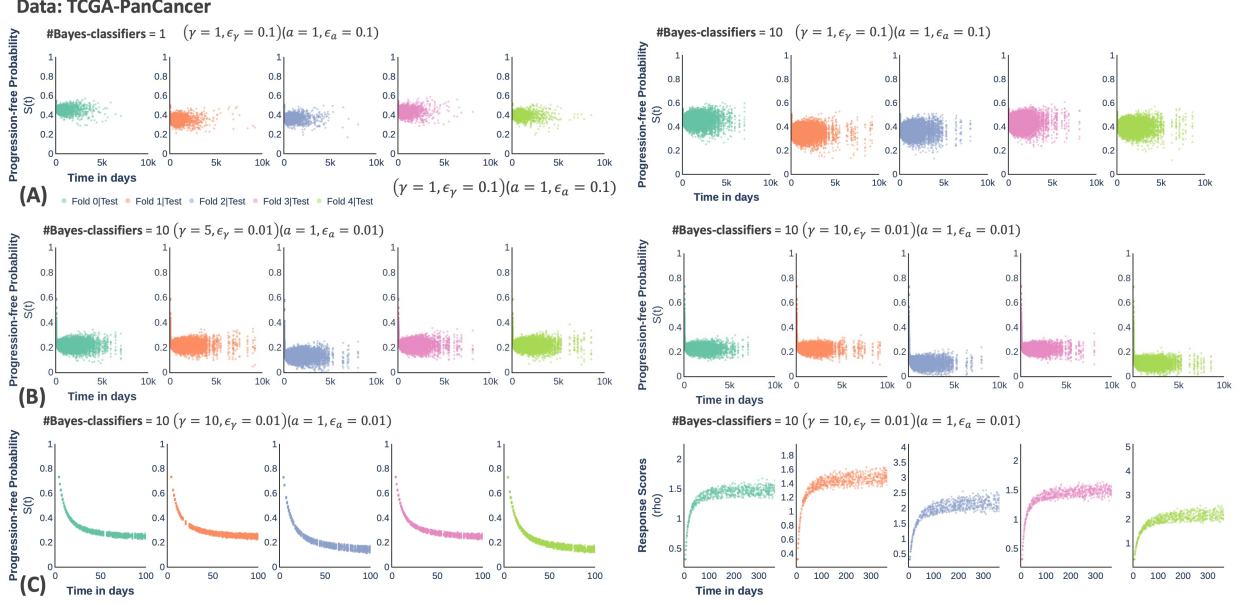


Figure 5: The Bayesian Inference of Proposed Model for PFS probability of Pan-Cancer Analysis from TCGA Database.

with input targets $I_i = (t_i, e_i)$, t_i is the monitored time and e_i is the indicator of progression/not-progression.

I employ objective-oriented surrogate optimization [3] to produce Bayesian classifiers for the quantified problem, similar to my previous work [13]. Specifically, I assume that for a given survival data set $D = \{I_i\}$, there will be optimal $(\gamma, \epsilon_\gamma)$ and $(\alpha, \epsilon_\alpha)$, such that with

$$\begin{aligned} \gamma &\leftarrow \mathcal{U}[\gamma - \epsilon_\gamma, \gamma + \epsilon_\gamma] \\ \alpha &\leftarrow \mathcal{U}[\alpha - \epsilon_\alpha, \alpha + \epsilon_\alpha] \end{aligned} \quad (9)$$

yields maximum concordance index (c-index) in **Equation 8** with \mathcal{U} is the uniform distribution. I use Bayesian optimization with Tree Parzen Estimator for model optimization, which enables efficient model hyper-parameters and parameter optimizations in massive search space [3]. Implementing the proposed quantum algorithm is efficient, enabling training using Graphical Processing Units (GPU). Besides, the experimental environment is limited computational hardware, with GeForce GTX 1060 Mobile GPU and 6GB memory. All experiments was carried out using Python 3.7.0, numpy 1.21.5, scikit-learn 1.0.2, and PyTorch 1.11,

4 Results

4.1 Case-study

I demonstrate the proposed model using The Cancer Genome Atlas databases [1], with 10,907 fully reported PFS data. The event indicator is 1 for a patient having a new tumor, which can be due to disease progressions, local recurrence, distance metastasis, or a new primary tumor appearing in any site; otherwise, the data is censored. Of note, the PFS is recommended by the data provider for a relatively short follow-up time. Thus, I will use **days** for the unit of time in further analysis. Besides, I validate the model by 5-fold cross-validation, meaning the model is trained on 80% of the data and tested on the separated remaining 20% of the given set.

4.2 Pan-Cancer Analysis of Progression-free Probability

I report the Bayesian inference of the proposed model for PFS probability of Pan-Cancer analysis using the TCGA database in **Figure 5**. By adopting Bayesian optimization for my work, I can produce an arbitrary number of classifiers derived from the learned distribution of model weights to amplify the confidence of model prediction as 1 and 10 classifiers. With the same set of model parameters, more classifiers ($n = 10$) propose larger confident regions for model prediction, which covers the case of smaller number classifier ($n = 1$). Besides, the distribution is shifted, corresponding to increasing trap strength from 5 to 10 (conceptualized) units, depicted in the middle panel.

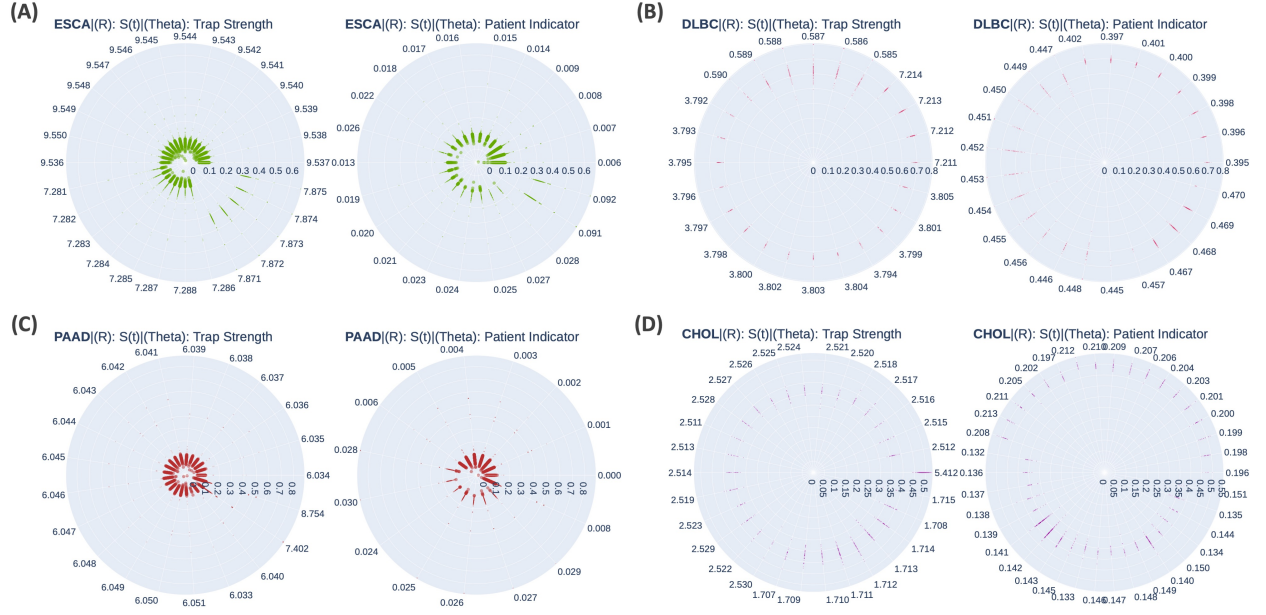


Figure 6: Disease-Specific T.A.R.G.E.T Plots for Model Interpretation.

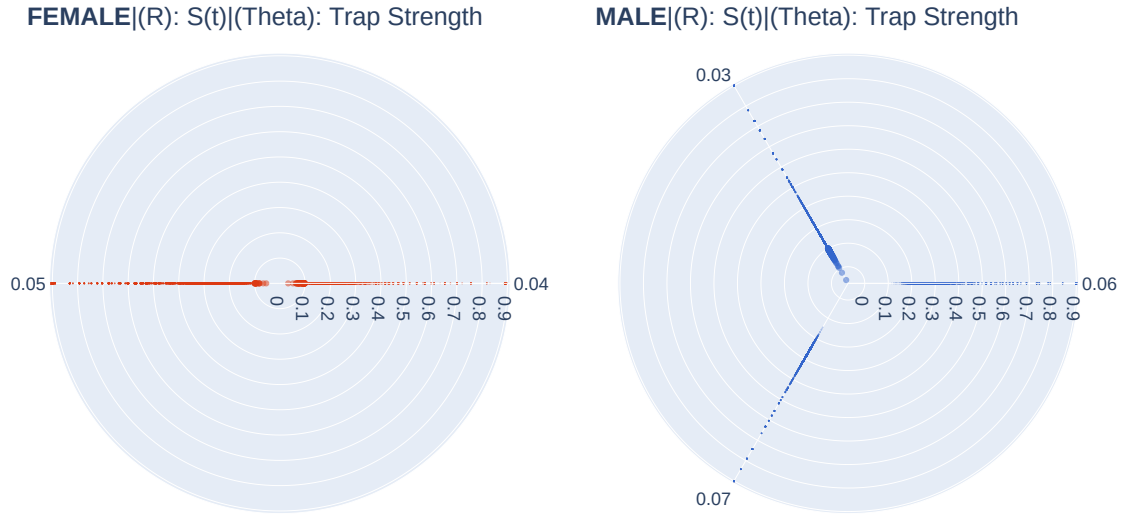


Figure 7: Gender-Specific T.A.R.G.E.T Plots for Model Interpretation.

I see a strangeness in the proposed model prediction surface due to the quantum diffusion. Specifically, the proposed model prediction suggests the PFS probability of the patient is aggressively reduced within only 100 days after the monitored time. After this time frame, the model suggests that the predicted chance of tumor progression is randomly distributed surrounding certain values, ranging from 0.2 – 0.4.

Although showing the stranger dynamics due to quantum diffusion, the model prediction is consistent with the KM model (Figure 1). Specifically, after 5,000 days, the model in Figure 5, top-left panel suggests the PFS chance is around 50%, slightly higher than the KM model, which means such probability beyond 5,000 days is under roughly 40% (Figure 1). The gap between the two models is closed as the monitored time reaches the endpoint. Specifically, the KM model suggests that such probability is around 0 to 0.2 at approximately 10,000 days (≈ 27 years). The same observations can be drawn from the middle panel of Figure 5, in which model predictions at the endpoint are randomly diffused around 0 in the second fold with trap five units; 0.2 in the second and the fmyth fold with trap ten units; and 0.2 in the remaining folds.

By linking the PFS chance with response scores via negative correlations, I can estimate the response scores of the entire TCGA PanCancer cohort forward in time. Interestingly, the dynamics of proposed response scores are like utility functions used in actuarial science [6] or von Bertalanffy growth [14]. Specifically, the proposed model suggests that the response effect of treatment may significantly increase from 0 to approximately $[1.2 - 2.0]$. At the diffusion time after 100 days, the response effects are saturated and plateau at some values. These plateau effects biologically make sense since treatment effects could decay as the drug is decayed by exposure to the tumor. For example, the treatment response score stops growing significantly after 100 days of the first year, and this effect gradually increases within the remaining 256 days. Using relatively short time-to-event data can be a pattern to construct treatment-response modeling for long-term treatment planning. Specifically, given two observations collected on days 100 and 200, I can estimate the response score by the end of the day 365 by knowing the functional surface’s general dynamics representing model predictions.

4.3 Sub-Group-Specific Analysis

Disease-specific Analysis: I propose T.A.R.G.E.T plots to interpret the proposed quantum survival model in **Figure 6** and **7**. Recall that I hypothesize that the tumor (particle) survival chance can be modeled via the quantum mechanism of trapping quantum particles on the 1D chain. I link this physically-inspired mechanism to the plot, where it can be imagined that a trap is placed at the center of the plot, enticing particles coming from different configurations of models. This variational learning explains model prediction via the two proposed-hypothesized indicators, including trap strength (presented on the radial unit (theta) surrounding the plot). The proposed model interpretation reveals intrinsic patterns from the survival chance of tumor, stratified by diseases. Samples with PFS chance below 0.1 is depicted in bigger markers (**Figure 6**). Some cancer phenotypes present better response scores to treatment, i.e., higher PFS, like DLGB or CHOL. In contrast, ESCA and PAAD have more aggressive behaviors to treatment since more samples with PFS probability below 0.1.

Gender-specific Analysis: I can use T.A.R.G.E.T plot to compare the behavior of tumors stratified by genders in **Figure 7**. the proposed model suggests that female tends to have a narrow range for the trap strength to reduce the PFS below 0.1 effectively, ranging from 0.04 to 0.05 with discretized two digits after the fractions. In contrast, male patients are stratified into two subgroups, effectively treated at 0.03 and ineffective regions between 0.06 and 0.07. This observation suggests that treatments for females require stronger effects (larger trap strength) than male treatment to reduce the PFS chance of tumor below 0.1.

5 Conclusion

To this end, I have presented a quantum survival model in the context of treatment response modeling and outlined the theory and concept behind it in **Sections 2.2** and **3.1**. I have also introduced an efficient training protocol for this model on advanced computing hardware in **Section 3.4**. I have applied the model to a practical case study involving Big Data of Pan-Cancer PFS analysis to demonstrate the proof of concept, as presented in **Section 4**.

My study suggests several avenues for further research. First, implementing the model on real quantum hardware could help to mitigate errors resulting from quantum simulation on classical computers and improve efficiency [5]. Second, exploring different configurations for the particle trap could address various treatment planning scenarios and is worth investigating in future work [2, 8, 12, 15]. Lastly, the proposed model is general and could be applied to other reliability analysis problems.

6 Acknowledgement

The author would like to thank all colleagues for stimulating and constructive comments.

References

- [1] D. C. C. B. R. . J. M. A. . K. A. . P. T. . P. D. . W. Y. 53 and T. S. S. L. D. A. 68. The cancer genome atlas pan-cancer analysis project. *Nature genetics*, 45(10):1113–1120, 2013.
- [2] C. Ampadu and G. Meltem. Survival probability of the quantum walk with phase parameters on the two-dimensional trapped lattice. 2013.
- [3] J. Bergstra, R. Bardenet, Y. Bengio, and B. Kégl. Algorithms for hyper-parameter optimization. *Advances in neural information processing systems*, 24, 2011.

- [4] C. Chandrashekar. Discrete-time quantum walk-dynamics and applications. *arXiv preprint arXiv:1001.5326*, 2010.
- [5] R. P. Feynman. Simulating physics with computers. In *Feynman and computation*, pages 133–153. CRC Press, 2018.
- [6] H. U. Gerber and G. Pafum. Utility functions: from risk theory to finance. *North American Actuarial Journal*, 2(3):74–91, 1998.
- [7] D. J. Griffiths and D. F. Schroeter. *Introduction to quantum mechanics*. Cambridge university press, 2018.
- [8] C. Huerta Alderete, S. Singh, N. H. Nguyen, D. Zhu, R. Balu, C. Monroe, C. Chandrashekar, and N. M. Linke. Quantum walks and dirac cellular automata on a programmable trapped-ion quantum computer. *Nature communications*, 11(1):3720, 2020.
- [9] E. L. Kaplan and P. Meier. Nonparametric estimation from incomplete observations. *Journal of the American statistical association*, 53(282):457–481, 1958.
- [10] J. P. Klein and M. L. Moeschberger. *Survival analysis: techniques for censored and truncated data*, volume 1230. Springer, 2003.
- [11] P. Krapivsky, J. Luck, and K. Mallick. Survival of classical and quantum particles in the presence of traps. *Journal of Statistical Physics*, 154:1430–1460, 2014.
- [12] A. A. Melnikov and L. E. Fedichkin. Quantum walks of interacting fermions on a cycle graph. *Scientific reports*, 6(1):1–13, 2016.
- [13] N. Nguyen and K.-C. Chen. Bayesian quantum neural networks. *IEEE Access*, 10:54110–54122, 2022.
- [14] L. Von Bertalanffy. Quantitative laws in metabolism and growth. *The quarterly review of biology*, 32(3):217–231, 1957.
- [15] P. Xue, H. Qin, and B. Tang. Trapping photons on the line: controllable dynamics of a quantum walk. *Scientific Reports*, 4(1):4825, 2014.